Research Article

Journal of Environmental Nanotechnology

A Study on the Magnetic Properties of Electrodeposited Cobalt-based Monolayer and Multilayer Alloys for Magnetic Sensor Application

Antonyraj Kanthiah[1*], Ezhil Inban Manimaran[2] and N. Vignesan[3]

[1]Department of Physics, Erode Sengunthar Engineering College, Erode, TN, India
[2]Department of Physics, Government Arts College, Coimbatore, TN, India
[3]Department of Physics, JCT College of Engineering and Technology, Coimbatore, TN, India
Received: 29.10.2025 Accepted: 01.12.2025 Published: 30.03.2026
*antonyrajphy@gmail.com

ABSTRACT

This work aims to investigate the magnetic characteristics of electrodeposited cobalt-nickel based monolayer and multilayer alloy coatings. The coatings were fabricated from chloride electrolyte with zinc and phosphorous incorporated to examine their influence on structural and magnetic behavior. Structural, and compositional analyses were carried out using X-Ray diffraction patterns, Field Emission Scanning Electron Microscope micrographs, and Energy Dispersive X-ray analysis. Magnetic properties were evaluated through hysteresis loop measurements and magnetoimpedance analysis. The results show that the incorporation of phosphorous in multilayer coatings affects the co-deposition of cobalt-nickel, leading to observable changes in microstructural features and magnetic behaviour compared with monolayer alloys. In particular, Co-Ni-P/Zn multilayer coating exhibits dependence of impedance on the applied magnetic field.

Keywords: Cobalt alloys; Multilayers; Dual-bath Technique; Electrodeposition; Phosphorous alloys; Magnetic alloys.

1. INTRODUCTION

Magnetic alloys and multilayers grabbed attention for several years because of their soft magnetic properties and their magnetic field sensing properties. Among various magnetic-field-sensitive phenomena, such as magnetoresistive effect and Hall effect, the giant magnetoimpedance (GMI) effect is extremely promising, displaying large impedance variations in soft magnetic materials under low magnetic fields. The GMI effect has been observed in cobalt-rich amorphous microwires, nanowires, thin films, ribbons, multilayers, bulk, and nanocomposites, making them suitable for sensing magnetic fields. Experimental studies on cobalt-based nanostructures revealed high sensitivity, low cost, fast response, low power consumption, and room-temperature operation. Hence, GMI effect-based magnetic sensors can be widely applicable in direction sensors, industrial and mining tools, nanoparticle detection, and biosensing systems (Zhukov *et al.* 2016; Oktaria *et al.* 2020; Da Silva *et al.* 2022; Liu *et al.* 2023; Gonzalez *et al.* 2025; Hrakova *et al.* 2025; Sammut and Calvi, 2025).

Alloys as monolayer and multilayer coatings were widely studied with the combination of many magnetic and non-magnetic elements (Sziráki *et al.* 2010; Shorowordi *et al.* 2017). Normally, these monolayer and multilayer alloys are prepared by evaporation, sputtering, and electrodeposition techniques (Sundaram *et al.* 2011; Tsyntsaru, 2016). Because of their complexity in fabrication, multilayer alloy coatings generally demand many parameters that need to be controlled and maintained. In particular, the formation of sequential layers and the incorporation of non-magnetic elements strongly encourage the nanostructure formation in the multilayers. Among other deposition techniques, the electrodeposition technique is regarded as the best method for preparing multilayers since it offers good control in sequential layer formation and purity (Landolt, 2002). The method also provides better physical properties such as corrosion resistance, magnetic properties, and electrochemical properties. Frequently, magnetic elements like cobalt, nickel, and iron-based alloys have been widely studied as binary, ternary, and multicomponent alloys with many non-magnetic elements to exploit their potential in supercapacitors, Hall effect sensors, and micro-electro-mechanical systems (MEMS) based on their microstructural and magnetic properties (Wang *et al.* 2010; Manimaran *et al.* 2018; Kalyani and Emerson, 2019; Zhang *et al.* 2019). To attain better electrochemical performance and magnetic properties, non-magnetic elements like tungsten, manganese, aluminium, copper, platinum, (Emerson *et al.* 2007) zinc (Liu *et al.* 2009; Pouladi *et al.* 2012; Shakoor *et al.* 2014; Tomic and Petrovic, 2015; Assaf *et al.* 2015) and phosphorous (Myung *et al.* 2003) were electrodeposited with these ferromagnetic elements. In contrast to monolayer alloy coatings, multilayer coatings are often deposited using alternating magnetic and non-

magnetic elements, such as Co/Cu, Fe/Cr, which are known to exhibit giant magnetoresistance (GMR). Such magnetic properties of these multilayers are making them suitable for applications such as magnetoresistive sensors (Ross, 1994; Tokarz *et al.* 2010; Esmaili and Bahrololoom, 2012). This kind of multilayer was reported through two different methods, which are named single bath and dual bath techniques. Multilayers prepared using dual bath technique offer better uniformity in layer formation (Ross, 1994).

Electrodeposition of zinc incorporated magnetic alloys with Co, Ni, and Fe has been widely reported. These zinc-incorporated alloys with binary combinations have better anti-corrosive properties. So far, multilayer coatings consisting of cobalt and nickel have been prepared with single-bath and dual-bath electrodeposition techniques (Ross, 1994). However, zinc incorporated multilayers with the magnetic elements have been less reported. In the present work, the magnetic behaviour of the electrodeposited binary Co-Ni alloys, ternary Co-Ni-Zn alloys, and their multilayers with and without the inclusion of phosphorous has been compared and reported. The progression of the microstructure in zinc-incorporated monolayer and multilayer alloys was studied utilising an X-ray diffractogram. Elemental constituents and morphology in both alloys were investigated and confirmed using Energy Dispersive X-ray analysis (EDAX) spectrum and Field Emission Scanning Electron Microscopy (FE-SEM) micrographs. Cross-sectional micrographs have been used to verify the multilayer formation in the zinc-incorporated multilayers. Microhardness values of the binary, ternary, and multilayers have been studied with the help of the Vickers hardness method. Magnetic properties of the prepared samples were investigated using a hysteresis loop (M-H loop) with the help of a vibrating sample magnetometer at room temperature.

2. EXPERIMENTAL METHOD

Cobalt-based magnetic alloy coatings as monolayer and multilayer were electrodeposited by the galvanostatic technique. Chloride and sulphate-based electrolytes are commonly used in electrodeposition. However, chloride-based electrolytes generally yield deposits with higher metal content than sulphate bath, particularly in the case of Co and Ni deposition (Emerson *et al.* 2007; Manimaran *et al.* 2018; Kim *et al.* 2003). Hence, to attain cobalt and nickel-rich composition, both multilayers and monolayer alloy coatings were electrodeposited at room temperature using chloride-based electrolytes, which consisted of cobalt chloride, nickel chloride, potassium chloride, and zinc chloride. For the Co-Ni binary alloy deposition bath, a composition of 0.2 M of cobalt chloride, nickel chloride, and boric acid was used. The role of boric acid in the electrolyte is to stabilise the pH in the solution (Młynarek-Żak *et al.* 2025). The chosen chloride salts were dissolved in DI water. Copper sheets were used as the substrate, which were cleaned by acid dipping followed by an ultrasonic cleaning process.

2.1 Deposition of Co-Ni and Co-Ni-Zn Monolayer Alloys

Electrodeposition of a monolayer was performed at a current density of 10 mA/cm^2 for 30 minutes. This was selected as the optimum current density for uniform deposition. Lower current densities result in slow deposition and non-uniform layers, while higher current densities promote rapid growth, causing roughness and poor adhesion. The chosen current density balances deposition rate and ensures uniform monolayer formation. The Co-Ni-Zn deposition process was carried out using the listed chemicals in Table 1 at different zinc chloride concentrations (0.1 and 0.2 M). The deposition was carried out using the typical electrodeposition setup in which the cleaned copper plate (1.5 × 5 cm) was used as the cathode, and the cleaned nickel rod (1.5 × 5 cm) was used as the anode. After the deposition process, substrates were carefully removed from the bath, and the surface residues on the substrates were removed by washing with DI water.

Table 1. Bath composition used for Co-Ni-Zn monolayer alloy deposition

Monolayer Alloy	Concentration	Ingredients in Bath
Co-Ni-Zn	0.2 M	Cobalt chloride Nickel chloride Boric acid Potassium chloride
	0.1 (or) 0.2 M	Zinc chloride

2.2 Deposition of Multilayers

Co-Ni/Zn and Co-Ni-P/Zn multilayers were deposited on the copper substrate using a dual bath technique, from two separate electrolyte baths (Podlaha *et al.* 2007). Similar to monolayer, multilayers were also deposited on the cathode (Cu plate) using nickel as the anode. It was placed in a specially designed holder, which makes the manual transfer very simple. The dual-bath deposition process used for multilayer preparation is illustrated in Fig. 1, and the bath composition used for the deposition is given in Table 2.

Conventionally, phosphorous-doped alloys exhibit good refinement in microstructural and compositional characteristics, which eventually play a vital role in magnetic properties. In the present work, doping of phosphorous content at a low percentage in the multilayer was achieved by adding sodium hypophosphite to the Co-Ni bath (Cojocaru *et al.* 2010). In multilayer deposition, the thickness of each layer is primarily controlled by the deposition time in each electrolyte bath, while the current density further regulates the final multilayer structure. Unlike

monolayer, multilayer deposition was carried out in different current densities, 10 mA/cm^2 for bath-1 and 5 mA/cm^2 for bath-2. In the multilayer deposition process, the zinc layers were deposited at a low current density. When the current density for zinc deposition is increased, zinc layer becomes thick and has poor adhesion. Therefore, zinc deposition was performed at low current density to maintain controlled and adherent layer formation. Deposition of individual layers is attained by transferring the substrate over two baths, while the substrates were dipped in DI water to remove deposition residues in the sequential layers. After the completion of multilayer deposition, the substrates were washed with DI water as mentioned earlier in monolayer deposition, and then characterized.

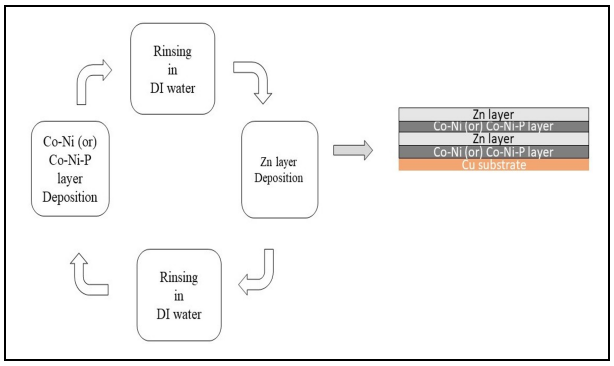


Fig. 1: Electrodeposition process of multilayers

Table 2. Bath composition used for multilayer deposition

Multilayers	Ingredients in Bath-1 (0.2M)	Ingredients in Bath-2 (0.1M)
Co-Ni/Zn Multilayer	Cobalt chloride Nickel chloride Boric acid	Zinc chloride Potassium chloride Boric acid
Co-Ni-P/Zn Multilayer	Cobalt chloride Nickel chloride Sodium hypophosphite Boric acid	Zinc chloride Potassium chloride Boric acid

3. RESULTS AND DISCUSSION

3.1 Chemical Composition in the Deposited Layers

To define the elemental composition of the electrodeposited samples, EDAX analysis was carried out for the coatings prepared from the optimised operational parameters. EDAX analysis was performed on the top surface of the electrodeposited coatings, which is the side facing the anode and represents the functionally active area. Fig. 2 – 5 show the EDAX spectrum of the electrodeposited alloy coatings. All the samples were found to have relevant elements with oxygen formation; the presence of oxygen in the coatings was contributed by the electrolytes. The presence of copper peaks was observed due to the usage of copper substrates (Resali *et al.* 2013; Kalyani and Emerson 2019). The total element percentage of Co and Ni in the multilayer was better for both multilayers compared to monolayers. The zinc element percentage in multilayers was found to be nearly 20-35 %. This reduction is due to the enriched Co-Ni layer deposition compared to Zn layers. At the optimised current density, Co and Ni show faster kinetic reduction rates than Zn, so the available cathodic current is preferentially directed to Co and Ni-rich alloy formation, leading to suppressed Zn deposition.

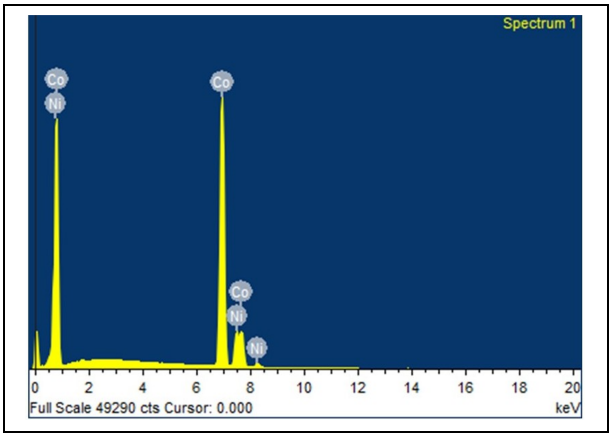


Fig. 2: EDAX spectrum of Co-Ni alloy

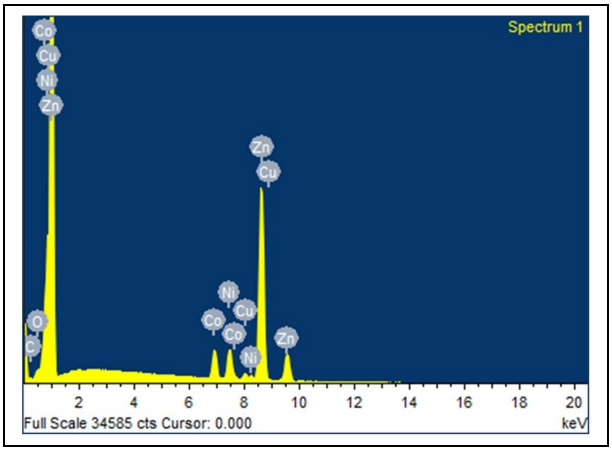


Fig. 3: EDAX spectrum of Co-Ni-Zn alloy deposited from the bath with 0.1M zinc chloride concentration

3.2 Morphological Analysis

Morphological variations in the electrodeposited alloy coatings were studied using FESEM micrographs. Fig. 6 (a-c) shows the micrographs of monolayer alloys. Co-Ni alloy coatings exhibit strong dendritic structures. Co-Ni-Zn alloy coatings prepared from the bath with 0.1 M zinc chloride concentration were found to be uniform and crack-free deposits. Fig. 6 (b) reveals the deposition of fine-granules and dense deposits in the monolayer. When the same combination was deposited as Co-Ni/Zn multilayer, the micrographs confirm the development of flake-like structure and

confirm the deposition of less dense zinc layers over the Co-Ni layers (Fig. 7(a)). The zinc layer is identified by its characteristic flake–like morphology, which contrasts with the finer texture of the Co-Ni layer. Cross-sectional micrograph of Co-Ni/Zn is shown in Fig. 7(b) which shows uniformly formed individual layers. Morphology of phosphorous influenced Co-Ni-P/Zn multilayer (Fig. 8(a)) indicates the deposition of a uniform Co-Ni-P layer and much larger zinc particles than the Co-Ni/Zn multilayer, which results in the formation of large particles. As can be seen from the figures, all the coatings were completely covered over the substrate without any pores. Additionally, in both multilayers, zinc layers have less homogeneity than the Co-Ni and Co-Ni-P layers. Although Zn is deposited at a lesser current density, even a minor surge in its deposition rate can produce uneven growth, making the Zn layer inhomogeneous above the Co–Ni layer. The Zn layer seems less dense and less homogeneous on the Co-Ni-coated substrate because the different current densities used for each layer change the nucleation rate of the Zn layer. Cross-sectional micrograph of Co-Ni-P/Zn multilayer is shown in Fig. 8(b), which shows that all the individual layers were formed uniformly. In phosphorous-doped layers, the Zn layers were detectable much more easily than in multilayers prepared without phosphorous.

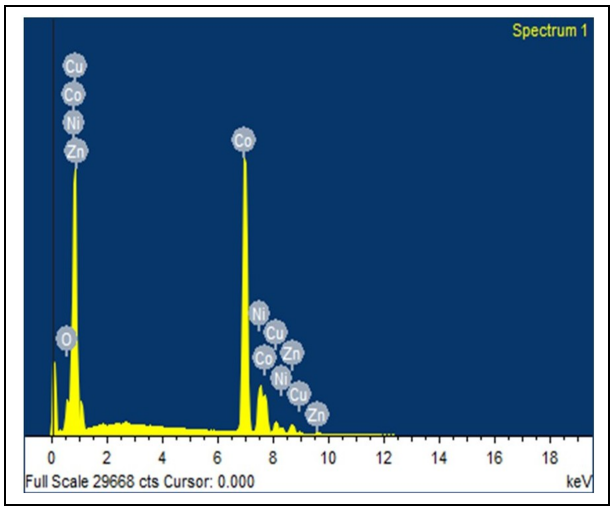


Fig. 4: EDAX spectrum of Co-Ni/Zn multilayer

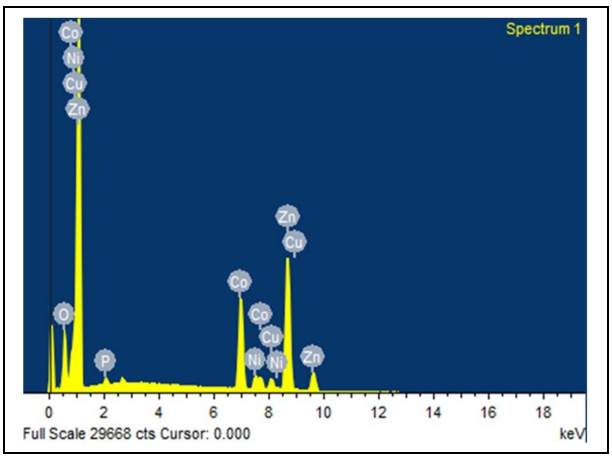


Fig. 5: EDAX spectrum of Co-Ni-P/Zn multilayer

3.3 Structural Characterization

To highlight the possible variations in structural properties, X-ray diffraction analysis was done on the electrodeposited samples. Fig. 9 (a – d) shows the XRD pattern of Co-Ni, Co-Ni-Zn alloys, and multilayers attained at the optimized deposition parameters. The obtained data from the XRD pattern confirm that the incorporation of zinc in Co-Ni-Zn improved the crystalline nature compared to the Co-Ni binary alloy. However, in the Co-Ni/Zn multilayer, a slight variation was observed in the crystalline nature, which shows a milder amorphous nature than the Co-Ni-Zn monolayer. The diffraction peaks were indexed to mixed phases, with dominant reflections from the (200) and (220) planes in monolayer and multilayer alloys, which correspond to the 2θ value of 50° and 74°. Multilayer samples have mixed FCC and HCP phases. The XRD pattern in Co-Ni-P/Zn shows distinct diffraction peaks corresponding to the (111), (200), and (220) planes. Peak narrowing in the (200) and (220) planes indicate improved crystallinity. The grain size of the prepared coatings was estimated using the Scherrer formula (Table 3) and was found to be in the range of nanometers. Grain size of the Co-Ni-P/Zn multilayer coatings was found to be increased due to the deposition of zinc at a high deposition rate over the Co-Ni-P layer, which leads to large particle formation.

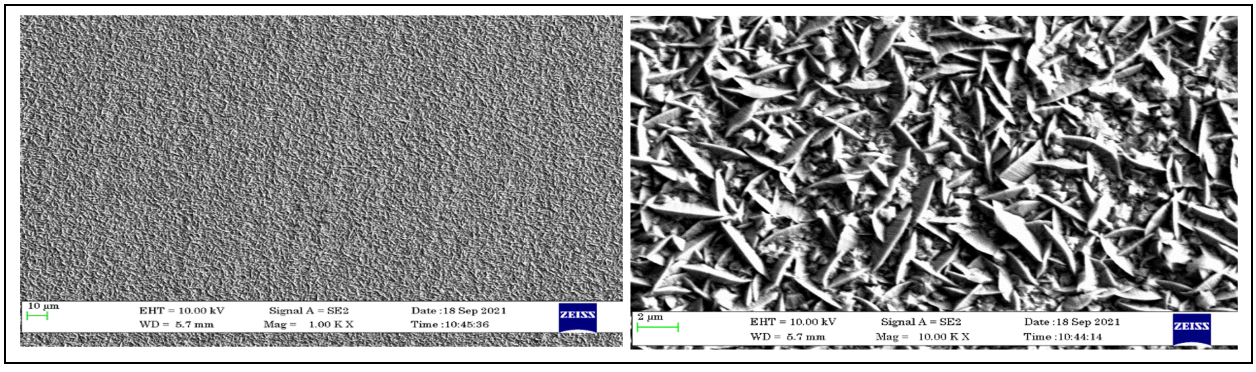


Fig. 6 (a): FE-SEM micrographs of the Co-Ni alloy

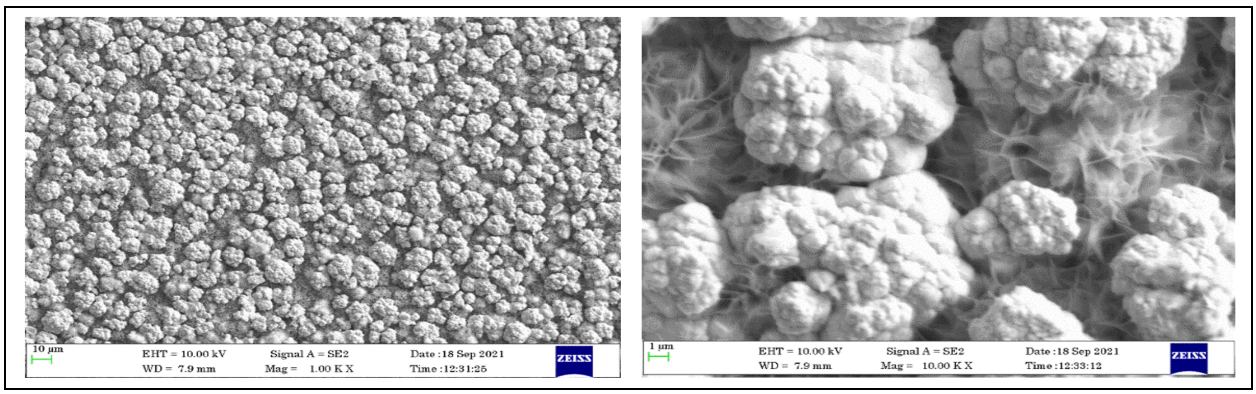


Fig. 6 (b): FE-SEM micrographs of the Co-Ni-Zn alloy deposited from the bath with 0.1 M zinc chloride

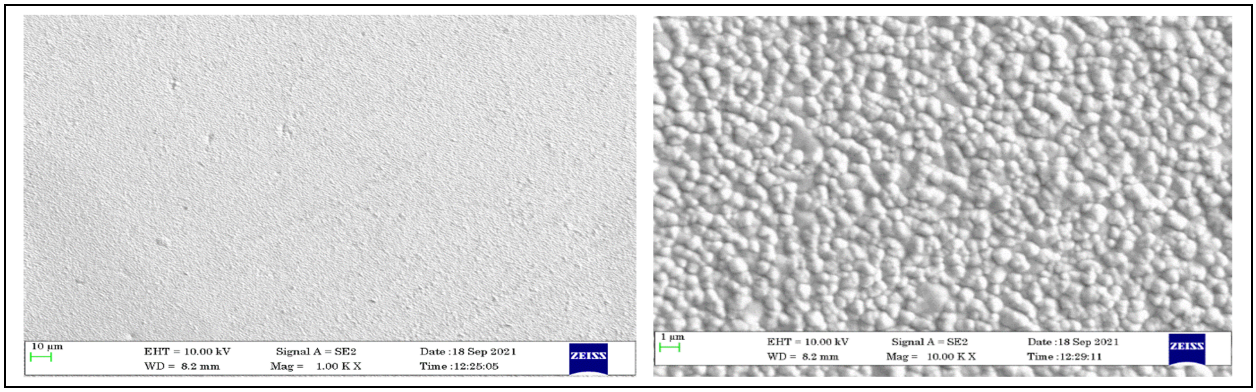


Fig. 6 (c): FE-SEM micrographs of the Co-Ni-Zn alloy deposited from the bath with 0.2 M zinc chloride

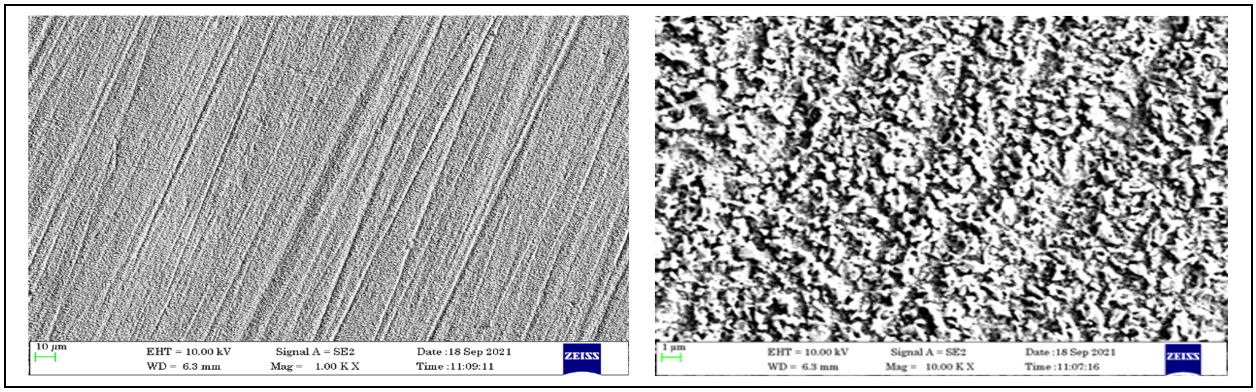


Fig. 7 (a): FE-SEM micrographs of the Co-Ni/Zn multilayer

3.4 Magnetic Studies

Magnetic properties of the prepared samples were investigated using an M-H loop with a vibrating sample magnetometer at room temperature (Fig.10 (a – c), 11(a & b), Table 4). It is well known that the magnetic properties of a magnetic alloy are highly dependent on its microstructure. In the present work, the Co-Ni-Zn monolayer prepared from the bath with 0.2 M zinc chloride exhibits an abrupt soft magnetic nature, due to the dominance of Ni and Zn content. Except for these coatings, all other coatings exhibit improvement in coercivity compared to Co-Ni alloys. When zinc incorporation was achieved in monolayer coatings, the M-H response gives a higher saturation than other zinc-incorporated coatings. However, the coercivity was found to be improved for multilayers. Due to the development of well-defined large particles (Fig. 8 (a)) with good crystallinity, the coercivity of the samples was drastically improved to 1065 Oe for Co-Ni-P/Zn multilayer compared to Co-Ni/Zn multilayer with 291 Oe. The Co–Ni-Zn monolayer alloys exhibit high magnetic saturation values because of their well-developed crystalline structure, but their coercivity remains low since the larger grains provide restricted barriers to domain-wall motion. In contrast, the

phosphorous incorporated multilayers exhibit higher coercivity because phosphorous leads to cobalt, nickel co-deposition and the formation of finer grains, which enhances the magnetic hardness in Co-Ni-P/Zn multilayers. Similar to previously reported works, ferromagnetic behaviour in all alloy coatings was found to be dependent on their elemental composition and microstructural properties. (Byun *et al.* 1993; Emerson *et al.* 2007; Sun *et al.* 2011).

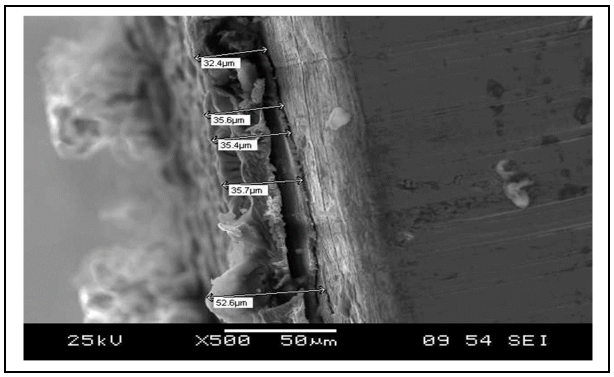


Fig. 7 (b): FE-SEM cross-sectional micrographs of the Co-Ni/Zn multilayer

Table 3. Structural properties of the monolayers and multilayers

Sample	Grain Size (nm)
Co-Ni monolayer alloy	15
Co-Ni-Zn monolayer alloy (0.1 M zinc)	21
Co-Ni/Zn multilayers	13
Co-Ni-P/Zn multilayers	20

3.5 Hardness properties

The microhardness of the electrodeposited samples was analysed with the help of a microhardness tester. Table 5 presents the microhardness of the electrodeposited alloys and multi-layered alloy coatings. It can be observed that the microhardness value of the Co-Ni binary alloy was 148 VHN. In zinc incorporation, the microhardness was decreased to 118 VHN. This reduction is due to the addition of zinc in Co-Ni elements. In phosphorous-added multilayers, this was steadily improved to 121 VHN. In CoNiP/Zn multilayers, phosphorous increases hardness by refining the layer structure and strengthening each layer, making the overall multilayers more rigid. When the multilayers were subjected to microhardness evaluation, the diamond indenter used for the analysis had gone through a different number of layers than monolayers, which shows that hardness values were also dependent on the number of layers and the elements in a sample (Panagopoulos *et al.* 2019). In this present work, the hardness values were highly reliant on the alloying element (Zn), which reduces the hardness values in ternary alloys and multilayers compared to Co-Ni alloys.

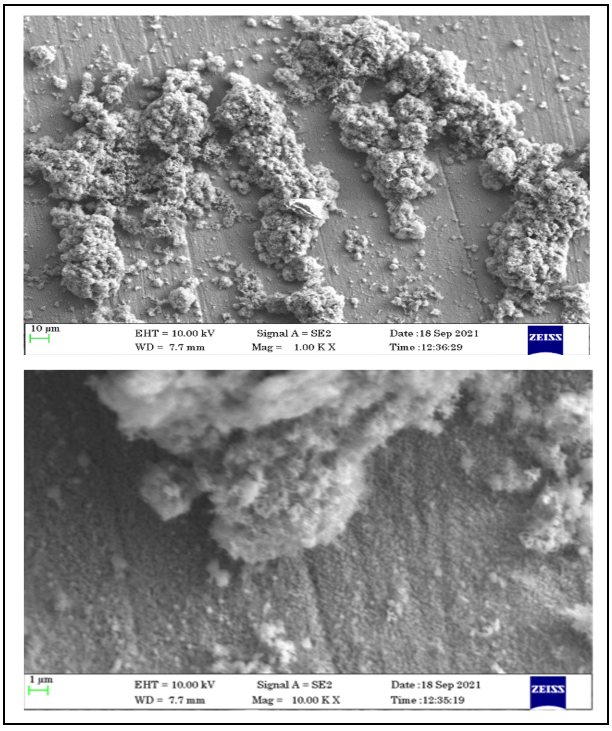


Fig. 8 (a): FE-SEM micrographs of the Co-Ni-P/Zn multilayer

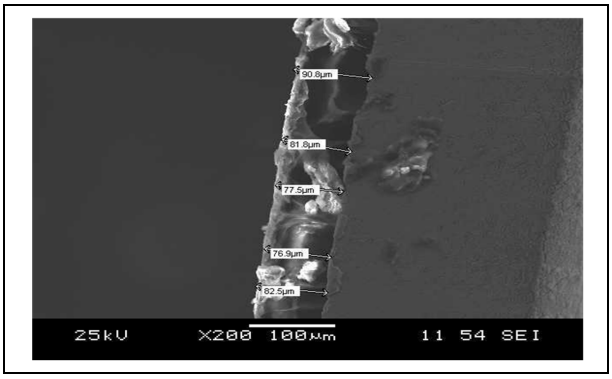


Fig. 8 (b): FE-SEM cross-sectional micrographs of the Co-Ni-P/Zn multilayer

Table 4. Magnetic properties of the monolayers and multilayers

Sample	M_r emu	M_s emu	Coercivity Oe
Co-Ni alloy	0.16643	0.39110	214
Co-Ni-Zn Monolayer Alloy			
0.1 M zinc	20.153×10^{-3}	58.762×10^{-3}	226
0.2 M zinc	646.05×10^{-6}	8.6910×10^{-3}	114
Multilayers			
Co-Ni/Zn	2.2476×10^{-3}	42.056×10^{-3}	291
Co-Ni-P/Zn	4.3761×10^{-3}	28.561×10^{-3}	1065

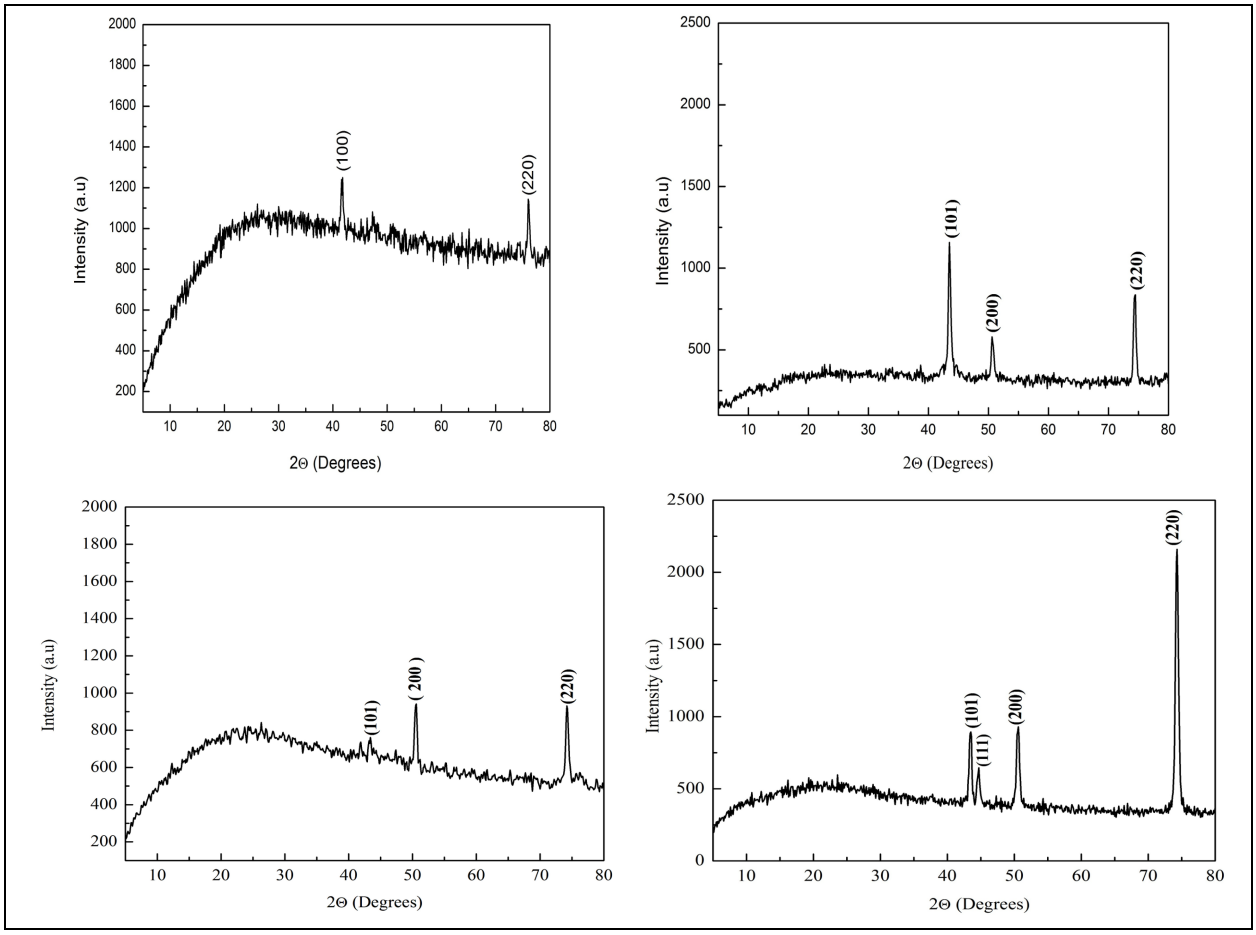


Fig. 9 (a) XRD pattern of the Co-Ni alloy (b) XRD pattern of the Co-Ni-Zn alloy deposited from the bath with 0.1 M zinc chloride (c) XRD pattern of the Co-Ni/Zn multilayer and (d) XRD pattern of the Co-Ni-P/Zn multilayer

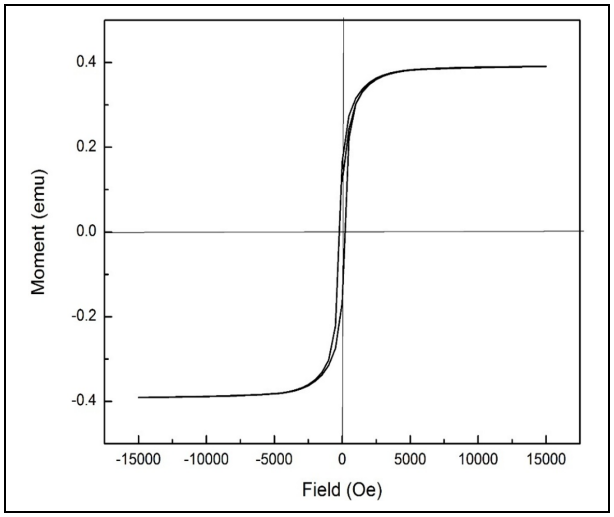


Fig. 10 (a): Hysteresis loop of the Co-Ni alloy

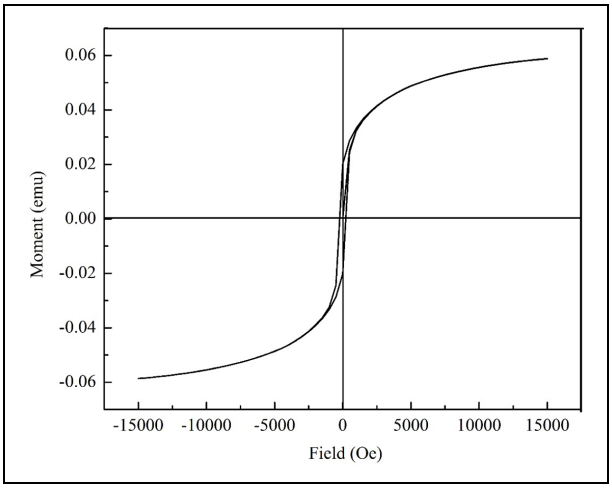


Fig. 10 (b): Hysteresis loop of the Co-Ni-Zn alloy deposited from the bath with 0.1 M zinc chloride

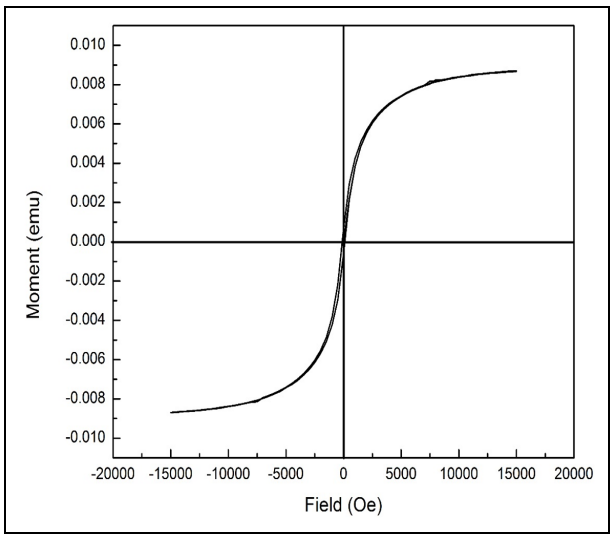


Fig. 10 (c): Hysteresis loop of the Co-Ni-Zn alloy deposited from the bath with 0.2 M zinc chloride concentration

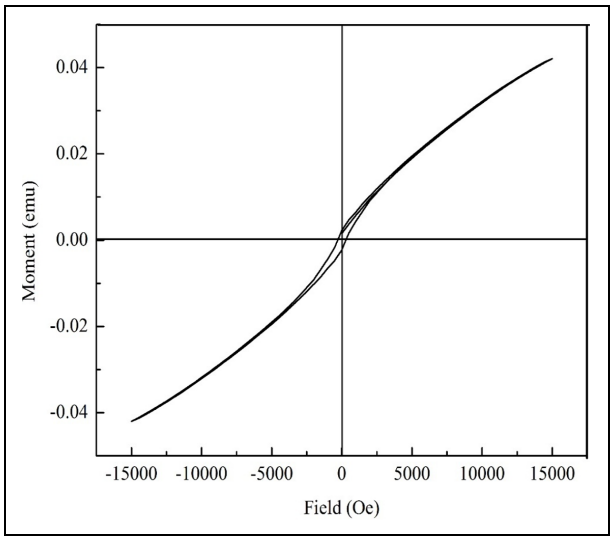


Fig. 11(a): Hysteresis loop of Co-Ni/Zn multilayer

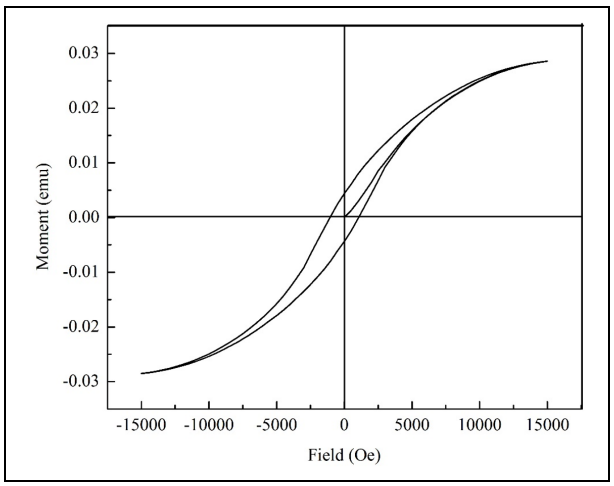


Fig. 11(b): Hysteresis loop of Co-Ni-P/Zn multilayer

Table 5. Hardness properties of the monolayer and multilayers

Alloys	Vickers Hardness (VHN)
Co-Ni Monolayer	148
Co-Ni-Zn Monolayer (0.1 M Zn)	118
Co-Ni/Zn Multilayer	117
Co-Ni-P/Zn Multilayer	121

3.6 Magnetoimpedance Studies

The magnetic sensitivity of the electrodeposited samples was confirmed by analyzing their magnetoimpedance properties. Fig. 12 shows the experimental setup used for magnetoimpedance. The magnetoimpedance analysis was performed by placing the electrodeposited samples with the dimensions of 1.5 × 5 cm inside a solenoid coil, which was magnetized using an external current source. It was positioned parallel to the applied magnetic field during the measurement. An impedance analyzer measured the impedance (Z) of the samples. The frequency of the A.C. current was kept constant, and the applied magnetic field (through solenoid coil) was varied to observe the deviation of impedance (Z) concerning the applied field. The magnetic field was applied to the sample in the range of 10-200 Oe at room temperature, where the A.C. driving frequency for the measurement was constantly maintained as 200 kHz. Fig. 13(a-d) show the magnetoimpedance response of the electrodeposited sample for the applied magnetic field. From this, it is evident that the samples were magnetically sensitive in nature and impedance values were gradually decreasing as the magnetic field was increased. In the Co-Ni-P/Zn multilayer, the impedance values show a maximum deviation of 11 %. The magnetoimpedance response obtained in this study is consistent with previously reported responses for cobalt-based systems and it can be a potential candidate for magnetoimpedance sensors (Nishibe *et al.* 2000; Ribeiro *et al.* 2016; Xiang *et al.* 2019; Lopez *et al.* 2024).

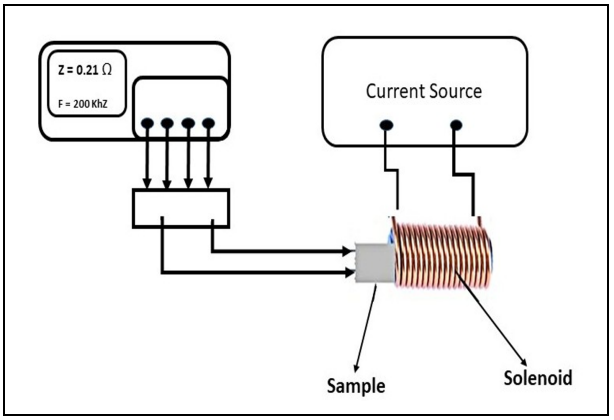


Fig. 12: Schematic representation of the experimental setup used for magnetoimpedance (MI) measurement

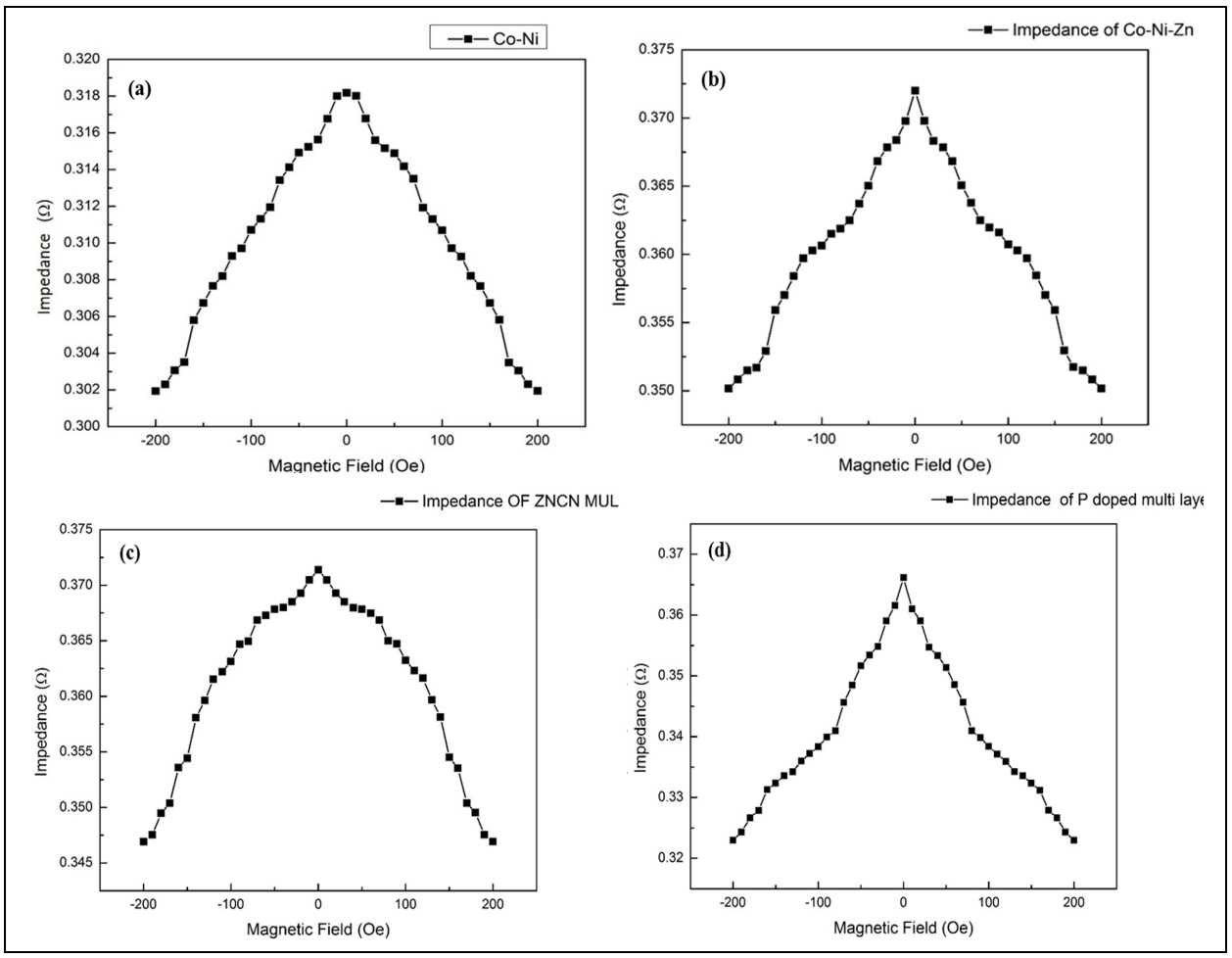


Fig. 13: Magnetoimpedance properties of electrodeposited (a) Co-Ni alloy (b) Co-Ni-Zn alloy from the bath with 0.1 M zinc chloride (c) Co-Ni/Zn multilayer (d) Co-Ni-P/Zn multilayer

4. CONCLUSIONS

Co-Ni, Co-Ni-Zn monolayer and Co-Ni/Zn, Co-Ni-P/Zn multilayer coatings were successfully fabricated using the electrodeposition technique. The inclusion of phosphorous in multilayers enhanced cobalt and nickel co-deposition, resulting in multilayers with improved microstructural uniformity and improved magnetic performance. Compared to monolayer and binary alloys, CoNiP/Zn multilayers exhibit higher coercivity (1065 Oe) and better overall magnetic characteristics. The magnetoimpedance analysis further confirms that Co-Ni-P/Zn multilayers exhibit distinctly higher impedance variation (11%). These improvements distinguish the developed multilayers from previously reported electrodeposited Co-Ni-based alloys.

Due to their improved magnetic properties, the Co-Ni-P/Zn multilayers prepared in this work show strong potential for use in magnetoimpedance-based sensors. Future work may explore the long-term magnetic ageing and stability to evaluate the durability and reliability of the multilayers for magnetoimpedance sensor applications.

FUNDING

This research received no specific grant from any funding agency in the public, commercial, or not-for-profit sectors.

CONFLICTS OF INTEREST

The authors declare that there is no conflict of interest.

COPYRIGHT

This article is an open-access article distributed under the terms and conditions of the Creative Commons Attribution (CC BY) license (http://creativecommons.org/licenses/by/4.0/).

REFERENCES

Assaf, F. H., El-Seidy, A. M. A., Abou-Krisha, M. M. and Eissa, A. A., Electrodeposition and Characterization of Zn-Ni-Mn Alloy from Sulfate Bath: Influence of Current Density, *Int. J. Electrochem. Sci.*, 10(7), 5465–5478 (2015). https://doi.org/10.1016/S1452-3981(23)17268-3

Byun, C., Rauch, G. C., Young, D. J., Klepper, C. A. and Greggi, J., Effects of hypophosphite contents and surface treatment on electroplated Co-Ni-P thin films, *J. Appl. Phys.*, 73(10), 5575–5577 (1993). https://doi.org/10.1063/1.353655

Cojocaru, P., Magagnin, L., Gómez, E. and Vallés, E., Electrodeposition of CoNi and CoNiP alloys in sulphamate electrolytes, *J. Alloys Compd.*, 503(2), 454–459 (2010). https://doi.org/10.1016/j.jallcom.2010.05.032

Da Silva, G. H. B., Ribeiro, P. R. T., Vilela, G. L. S., Raktkovisk, D. R., Abrão, J. E., Santos, E., Azevedo, A., Rodrigues, A. R., Padrón-Hernández, E., Rezende, S. M. and Machado, F. L. A., Investigation of the GMI effect in multilayered sensing elements deposited over silicon and glass substrates, *J. Magn. Magn. Mater.*, 560, 169678 (2022). https://doi.org/10.1016/j.jmmm.2022.169678

Emerson, R. N., Kennady, C. J. and Ganesan, S., Effect of organic additives on the magnetic properties of electrodeposited CoNiP hard magnetic films, *Thin Solid Films*, 515(7–8), 3391–3396 (2007). https://doi.org/10.1016/j.tsf.2006.09.034

Esmaili, S. and Bahrololoom, M. E., A new single bath for the electrodeposition of NiFe/Cu multilayers exhibiting giant magnetoresistance behavior, *Surf. Eng. Appl. Electrochem.*, 48(1), 35–41 (2012). https://doi.org/10.3103/S106837551201005X

Gonzalez, A., Corte-León, P., Zhukova, V., Blanco, J. M., Olivera, J. and Zhukov, A., Development of Co-rich glass-coated microwires with high GMI effect, *AIP Adv.*, 15(3), 035213 (2025). https://doi.org/10.1063/9.0000884

Hrakova, D., Asfour, A. and Ripka, P., Multi-modal GMI applications with annealed nanocrystalline core, *Meas. Sens.*, 38, 101424 (2025). https://doi.org/10.1016/j.measen.2024.101424

Lopez, A. R., Andrés, J. P., González, J. A., Garcia, G. A., Zhukova, V., Chizhik, A., Salaheldeen, M. and Zhukov, A., Tuning of magnetic properties and giant magnetoimpedance effect in multilayered microwires, *J. Sci. Adv. Mat. Dev.*, 9(4),100821 (2024). https://doi.org/10.1016/j.jsamd.2024.100821

Kalyani, M. and Emerson, R.N., Electrodeposition of nano crystalline cobalt oxide on porous copper electrode for supercapacitor, *J. Mater. Sci. Mater. Electron.*, 30(2), 1214–1226 (2019). https://doi.org/10.1007/s10854-018-0389-y

Daheum, K., Park, D. Y., Yoo, B. Y., Sumodjo, P. T. A. and Myung, N. V., Magnetic properties of nanocrystalline iron group thin film alloys electrodeposited from sulfate and chloride baths, *Electrochim Acta,* 48, 819-830(2003). https://doi.org/10.1016/s0013-4686(02)00773-9

Landolt, D., Electrodeposition Science and Technology in the Last Quarter of the Twentieth Century, *J. Electrochem. Soc.*, 149(3), S9 (2002). https://doi.org/10.1149/1.1469028

Liu, L., Li, H., Fan, S., Gu, J., Li, Y. and Sun, H., Fabrication and magnetic properties of Ni–Zn nanowire arrays, *J. Magn. Magn. Mater.*, 321(20), 3511–3514 (2009). https://doi.org/10.1016/j.jmmm.2009.06.062

Liu, M., Wang, Z., Meng, Z., Sun, X., Huang, Y., Guo, Y. and Yang, Z., Giant Magnetoimpedance Effect of Multilayered Thin Film Meanders Formed on Flexible Substrates, *Micromach.*, 14(5), 1002 (2023). https://doi.org/10.3390/mi14051002

Manimaran, E. I., Antonyraj, K., Navaneetha, E. R., Kumar, V. S. and Rajesh, P., Influence of different conducting substrates on magnetic properties of electrodeposited Ni–Fe thin films, *J. Mater. Sci. Mater. Electron.*, 29(5), 3715–3721 (2018). https://doi.org/10.1007/s10854-017-8304-5

Młynarek-Żak, K., Spilka, M., Matus, K., Góral, A. and Babilas, R., Electrodeposited CoFeNi Medium-Entropy Alloy Coating on a Copper Substrate from Chlorides Solution with Enhanced Corrosion Resistance, *Coatings*, 15(5), 509 (2025). https://doi.org/10.3390/coatings15050509

Myung, N. V., Park, D. Y., Yoo, B. Y. and Sumodjo, P. T. A., Development of electroplated magnetic materials for MEMS, *J. Magn. Magn. Mater.*, 265(2), 189–198 (2003). https://doi.org/10.1016/S0304-8853(03)00264-6

Nishibe, Y., Yamadera, H., Ohta, N., Tsukada, K. and Nonomura, Y., Thin film magnetic field sensor utilizing Magneto Impedance effect, *Sens. Actuators Phys.*, 82(1–3), 155–160 (2000). https://doi.org/10.1016/S0924-4247(99)00327-1

Oktaria, V., Utari, and Purnama, B., Influence of Multilayer Number to Magneto-Impedance Ratio in Electrodeposited $[NiFe/Cu]_N$ Multilayer, *Key Eng. Mater.*, 855, 191–196 (2020). https://doi.org/10.4028/www.scientific.net/KEM.855.191

Panagopoulos, C. N., Georgarakis, K. G. and Giannakopoulos, K. I., Zn–Fe multilayered alloy coatings produced by electrodeposition, *SN Appl. Sci.*, 1(1), 114 (2019). https://doi.org/10.1007/s42452-018-0120-x

Podlaha, E. J., Li, Y., Moldovan, M., Young, D. P., Wang, W. and Fan, R., Electrodeposition of Serpentine CoCu/Cu Multilayered GMR Micro-device, *ECS Trans.*, 2(6), 379–385 (2007). https://doi.org/10.1149/1.2408891

Pouladi, S., Shariat, M. H. and Bahrololoom, M. E., Electrodeposition and characterization of Ni–Zn–P and Ni–Zn–P/nano-SiC coatings, *Surf. Coat. Technol.*, 21333–40 (2012). https://doi.org/10.1016/j.surfcoat.2012.10.011

Resali, N. A., Hyie, K. M., Abdullah, W. N. R., Ghani, M. A. A. and Kalam, A., The Effect of Bath Ph on the Phase Formation of Ternary Co-Ni-Fe Nano-Coatings, *Appl. Mech. Mater.*, 3919–13 (2013). https://doi.org/10.4028/www.scientific.net/AMM.391.9

Ribeiro, P. R. T., Ramírez, J. M. M., Vidyasagar, R., Machado, F. L. A., Rezende, S. M. and Dahlberg, E. D., GMI in the reentrant spin-glass $Fe_{90}Zr_{10}$ alloy: Investigation of the spin dynamics in the MHz frequency regime, *Appl. Phys. Lett.*, 109(10), 102404 (2016). https://doi.org/10.1063/1.4962534

Ross, C. A., Electrodeposited Multilayer Thin Films, *Annu. Rev. Mater. Sci.*, 24(1), 159–188 (1994). https://doi.org/10.1146/annurev.ms.24.080194.001111

Sammut, N. and Calvi, M., Advances in Magnetic Sensors and Their Applications, *Sensors*, 25(17), 5590 (2025). https://doi.org/10.3390/s25175590

Shakoor, R. A., Kahraman, R., Waware, U. S., Wang, Y. and Gao, W., Synthesis and Properties of Electrodeposited Ni-B-Zn Ternary Alloy Coatings, *Int. J. Electrochem. Sci.*, 9(10), 5520–5536 (2014). https://doi.org/10.1016/S1452-3981(23)08186-5

Shorowordi, K. M., Moniruzzaman, M., Taufique, M. F. N. and Azam, A., Effect of Ni/Fe ratio of electrolyte salts on the magnetic property of electrodeposited Fe–Ni alloy, *Surf. Eng. Appl. Electrochem.*, 53(1), 52–58 (2017). https://doi.org/10.3103/S1068375517010124

Sun, X. M., Yuan, Q., Fang, D. M. and Zhang, H. X., Electrodeposition and characterization of CoNiMnP-based permanent magnetic film for MEMS applications, *IEEE Int. Conf. Nano/Micro Eng. Mol. Syst.,* 367–371 (2011). https://doi.org/10.1109/NEMS.2011.6017369

Sundaram, K., Raja, M., Thanikaikarasan, S., Chu, J. P. and Mahalingam, T., Role of pH and current density in electrodeposited soft magnetic Co-Ni-Fe alloy thin films, *Mater. Sci.-Pol.*, 29(3), 165–170 (2011). https://doi.org/10.2478/s13536-011-0037-1

Sziráki, L., Kuzmann, E., El-Sharif, M., Chisholm, C. U., Stichleutner, S., Lak, G. B., Süvegh, K., Tatár, E., Homonnay, Z. and Vértes, A., Electrodeposition of novel Sn–Ni–Fe ternary alloys with amorphous structure, *Appl. Surf. Sci.*, 256(24), 7713–7716 (2010). https://doi.org/10.1016/j.apsusc.2010.06.026

Tokarz, A., Wieczorek, P., Lis, A. and Morgiel, J., Microstructure of electrodeposited NiFe/Cu multilayers, *J. Microsc.*, 237(3), 456–460 (2010). https://doi.org/10.1111/j.1365-2818.2009.03293.x

Tomic, M. and Petrovic, M., Ternary Zn-Ni-Co alloy: Anomalous codeposition and corrosion stability, *J. Serbian Chem. Soc.*, 80(1), 73–86 (2015). https://doi.org/10.2298/JSC260814113B

Tsyntsaru, N., Electrodeposition of cobalt–tungsten alloys and their application for surface engineering, *Russ. J. Electrochem.*, 52(11), 1041–1047 (2016). https://doi.org/10.1134/S1023193516110136

Wang, H., Liu, R., Cheng, F., Cao, Y., Ding, G. and Zhao, X., Electrodepositing amorphous Ni-W alloys for MEMS, *Microelectron. Eng.*, 87(10), 1901–1906 (2010). https://doi.org/10.1016/j.mee.2009.11.018

Xiang, S., Zou, J., Li, X., Xie, W. and Zhao, Z. J., Magnetic properties and giant magneto-impedance effect in electroless-deposited CoP/Cu composite wires, *Mater. Res. Exp.*, 6(6), 066101 (2019). https://doi.org/10.1088/2053-1591/ab0832

Zhang, Y., Hao, Q. and Xiao, G., Low-Frequency Noise of Magnetic Sensors Based on the Anomalous Hall Effect in Fe–Pt Alloys, *Sens.*, 19(16), 3537 (2019). https://doi.org/10.3390/s19163537

Zhukov, A., Talaat, A., Ipatov, M., Granovsky, A. and Zhukova, V., Estimation of the frequency and magnetic field dependence of the skin depth in Co-rich magnetic microwires from GMI experiments, *J. Sci. Adv. Mater. Devices*, 1(3), 388–392 (2016). https://doi.org/10.1016/j.jsamd.2016.08.002